Available online at www.sciencedirect.com
ScienceDirect
Polyhedron 25 (2006) 3463–3473
POLYHEDRON
www.elsevier.com/locate/poly

# Complexes of pendant-armed cyclam derivatives with copper(II) perchlorate: Synthesis and crystal structures

Thomas Schönherr, Wilhelm Seichter, Edwin Weber *

*Institut für Organische Chemie, Technische Universität Bergakademie Freiberg, Leipziger Strasse 29, 09596 Freiberg/Sachs., Germany*

Received 17 January 2006; accepted 22 June 2006
Available online 14 July 2006

**Abstract**

A designed series of cyclam type macrocyclic ligands **1**–**3** that feature a different degree of saturation and number of functional appendages of the macroring, including preparation of the respective Cu(II) perchlorate complexes **1a**–**3a**, was synthesized. Comparative discussion of the X-ray crystal structures of the free ligands and the corresponding complexes shows that dependent on the structure of the compound, transanular, pendant arm and anion involving conventional and weaker H bond contacts are operating. In the complexes, the coordination environment around the Cu(II) cation is distorted octahedral with the nitrogens of the macroring defining the equatorial sites and either two oxygens, each of a perchlorate anion, or the lateral pyridine nitrogens in apical positions. Thus, only the pyridine containing pendants in **3a** proved effective in metal ion coordination while the anisyl groups are engaged in H bonding, respectively. The uncomplexed macrocycle **3** yielded an inclusion compound with chloroform, also indicating a special ability relating to this series of compounds.


*Keywords:* Copper; Co-ordination compounds; Macrocyclic ligands; Cyclam derivatives; Crystal structures

## 1. Introduction

Macrocycles containing nitrogen donor atoms are an important class of compounds due to their prominent behavior of forming highly stable complexes with a variety of transition metal ions [1,2]. Oligoaza macrocycles were also found effective receptor molecules for ammonium cations [1,3], and in its protonated or quaternary form they are tried and tested in the formation of complexes with anionic guests [4]. In recent years, growing interest is being attached to the functionalization of oligoaza macrocyclic ligands [5–7], producing pendant-arm complexes [8,9] that show high catalytic potential [10]. Complexes of this type can stabilize unusual oxidation states of coordinated transition metal ions, making them a promising tool for the construction of supramolecular switches [11], while open framework structures, generated from respective complexes as the tectonic building block, are expected to yield sorptive materials for chemical sensing [12]. Moreover, an uncomplexed pendant-arm tetraaza macrotricycle was recently found to form a crystalline inclusion compound with chloroform [13].

From among the many different oligoaza macrocycles [14], 1,4,8,11-tetraazacyclotetradecane, commonly known as cyclam [15], is described as being the most classic example and useful representative of this type of compounds [16]. Currently, cyclam and its pendant-arm derivatives are extensively investigated in medicine for imaging applications [17] and as carriers of metal ions in antitumor [18] and anti-HIV agents [19], as well as in the construction of multifunctional dendrimers capable of coordinating metal ions [20].

Considering the promising aspects, we report in this paper on Cu(II) complexes of a designed series of cyclam type derivatives **1**–**3** (Scheme 1) featuring different degree of saturation of the macroring and different number of functional appendages involving C-linked 2-anisyl and

* Corresponding author. Fax: +49 3731 39 3170.
*E-mail address:* edwin.weber@chemie.tu-freiberg.de (E. Weber).

0277-5387/$ - see front matter © 2006 Elsevier Ltd. All rights reserved.
doi:10.1016/j.poly.2006.06.037

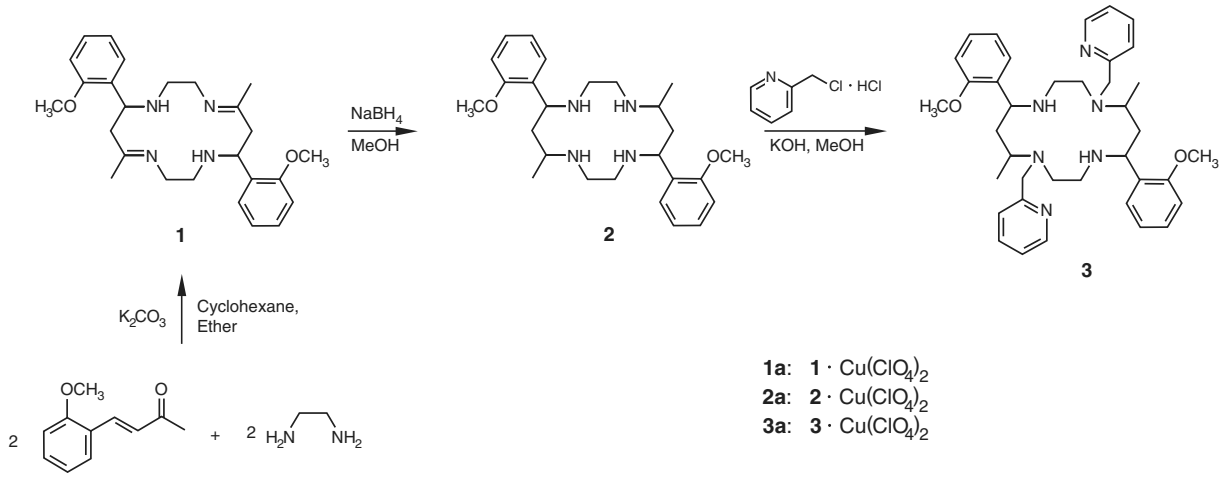


Scheme 1. Synthesis of the tetraaza macrocycles and specification of complexes studied.

N-linked 2-picolyl groups. Both, the crystal structures of all the uncomplexed macrocycles **1**–**3** and the respective Cu(II) complexes have been solved and comparatively discussed to reveal structural consequences on the coordination behavior. Thus, the present study will serve as a useful example of cyclam-type co-ordination chemistry being supplement to the known structures of related cyclams and cyclam complexes that differ in the absence of the methoxy substituents, respectively, anisyl pendants, or show other structural modifications [21–29].

## 2. Experimental

*Caution:* Although we did not encounter any problems, perchlorate salts of metal complexes containing organic ligands and solvents are potentially explosive and should be handled only in small quantities and with great caution!

### 2.1. General methods and materials

Melting points (uncorrected) were taken on a heating stage microscope (Rapido, Dresden). The IR spectrum ($\nu$ in $cm^{-1}$) was recorded on a Perkin–Elmer 1600 FT-IR instrument. NMR spectra ($\delta$ in ppm, $J$ in Hz, $Me_4Si$ as internal standard) were obtained with Bruker Avance DPX 400 ($^1H$: 400 MHz, $^{13}C$: 100.6 MHz). The mass spectrum (ESI) was determined on a Hewlett–Packard HP 59987 A instrument.

Reactions were monitored by thin-layer chromatography (TLC) carried out on Merck silica gel 60 F254 coated plates. All reagents were commercial products and were utilized without further purification. The solvents used were purified or dried by common literature procedures [30].

### 2.2. Synthesis of the macrocycles

2-Methoxybenzylideneacetone was obtained from 2-methoxybenzaldehyde and acetone according to the literature [31].

#### 2.2.1. 7,14-Bis(2-methoxyphenyl)-5,12-dimethyl-1,4,8,11-tetraazacyclotetradeca-5,12-diene (*1*)

Prepared from 2-methoxybenzylideneacetone and ethylenediamine with anhydrous potassium carbonate in cyclohexane–diethyl ether (1:2) following the literature procedure [27]. Recrystallization form chloroform–diethyl ether yielded 80% yellowish crystals; m.p. 144–145 °C (literature [32] m.p. 143–145 °C).

#### 2.2.2. 7,14-Bis(2-methoxyphenyl)-5,12-dimethyl-1,4,8,11-tetraazacyclotetradecane (*2*)

Synthesized by treatment of **1** with $NaBH_4$ in dry ethanol and workup according to the literature [32] which yielded 92% colourless crystals; m.p. 197–198 °C (literature [32] m.p. 198–199 °C).

#### 2.2.3. 4,11-Bis(2-pyridylmethyl)-7,14-bis(2-methoxyphenyl)-5,12-dimethyl-1,4,8,11-tetraazacyclotetradecane (*3*)

To a stirred solution of **2** (1.0 g, 2.43 mmol) and sodium hydroxide (0.44 g, 11.0 mmol) in water (20 $cm^3$) was added dropwise a solution of picolyl chloride hydrochloride in methylene chloride (20 $cm^3$). The mixture was stirred for 10 h at 25 °C. The organic phase was separated and the aqueous phase extracted with three 50 $cm^3$ portions of methylene chloride. The combined organic phases were evaporated under reduced pressure and the remaining oil crystallized from ethanol to give a colorless solid with m.p. 236–238 °C (yield: 82%). *Anal.* Calc. for $C_{38}H_{50}N_6O_2$ (FW = 622.85): C, 73.28; H, 8.09; N, 13.49. Found: C, 73.03; H, 8.19; N, 13.41%. IR (KBr): 3252, 2966, 2934, 2895, 2834, 2817, 1597 (s), 1588 (s), 1491 (s), 1472 (s), 1434 (s), 1364, 1274, 1237, 1135, 1084, 1050, 1029, 786, 766 (s), 756 (s) $cm^{-1}$. $^1H$ NMR ($CDCl_3$): $\delta = 0.96$ (s, 3H, $CH_3$), 0.98 (s, 3H, $CH_3$), 1.60–1.66 (m, 2H, C*H*–$CH_3$), 1.93 (b, 2H, NH), 2.29–2.90 (m, 12H, $CH_2$), 3.81 (s, 6H, $OCH_3$), 3.83 (m, 2H, NC*H*-Ar), 4.05 (s, 4H, $CH_2$-Ar), 6.86 (d, $J = 8.4$, 2H, Ar-H), 6.93 (m, 4H, Ar-H), 7.11 (d, $J = 6.8$, 2H, Ar-H), 7.20 (m, 2H, Ar-H), 7.59 (t,

$J = 3.6$, 2H, Ar-H),7.71 (d, $J = 7.2$, 2H, Ar-H), 8.47 (d, $J = 3.6$, 2H, Ar-H). $^{13}$C NMR ($CDCl_3$): $\delta = 13.8$ ($CH_3$), 40.5, 44.6 (CH*C*H$_2$CH, N*C*H$_2$*C*H$_2$N), 54.0, 54.6 (*C*HCH$_3$, *C*HAr), 55.3 ($OCH_3$), 56.1 (N*C*H$_2$Ar), 110.4, 120.7, 121.6, 123.2, 127.2, 127.4, 132.6, 157.1, 161.4 (Ar). MS (ESI): $m/z = 622$ ($M^+$).

### 2.3. Preparation of the $Cu(ClO_4)_2$ complexes

To a stirred solution of the corresponding macrocycle (0.7 mmol) in methanol (20 cm$^3$) was added $Cu(ClO_4)_2 \cdot 6H_2O$ (0.26 g, 0.7 mmol). The precipitate which had formed during 4 h was collected, washed with methanol and dried under vacuum.

***1*** $\cdot$ *Cu(ClO$_4$)$_2$ (**1a**)*: violet crystals (yield: 91%). *Anal.* Calc. for $C_{26}H_{36}Cl_2CuN_4O_{10}$ (FW = 699.04): C, 44.67; H, 5.19; N, 8.01. Found: C, 44.41; H, 5.21; N 7.94%. MS(ESI): $m/z = 598$ [M − ClO$_4^-$].

***2*** $\cdot$ *Cu(ClO$_4$)$_2$ (**2a**)*: dark-pink crystals (yield: 93%). *Anal.* Calc. for $C_{26}H_{40}Cl_2CuN_4O_{10}$ (FW = 703.07): C, 44.42; H, 5.37; N, 7.97. Found: C, 44.22; H, 5.78; N 7.91%. MS(ESI): $m/z = 601$ [M − ClO$_4^-$].

***3*** $\cdot$ *Cu(ClO$_4$)$_2$ (**3a**)*: blue crystals (yield: 95%). *Anal.* Calc. for $C_{38}H_{50}Cl_2CuN_6O_{10}$ (FW = 885.03): calcd. C, 51.56; H, 5.69; N, 9.49. Found: C, 51.45; H, 5.72; N, 9.38%. MS(ESI): $m/z = 783$ [M − ClO$_4^-$].

### 2.4. X-ray crystallography

In a general procedure, the addition of $Cu(ClO_4)_2 \cdot 6H_2O$ to an equimolar solution of the respective ligand (**1**–**3**) in methanol yielded the complexes **1a**–**3a** as amorphous powders. Further crystallization from selected solvents produced crystals suitable for X-ray crystallographic analysis. Crystallographic data of the complexes and those of the free ligands are summarized in Table 1.

X-ray diffraction studies of **1**, **2**, **2a**, **3** $\cdot$ 2CHCl$_3$ and **3a** were carried out on a Bruker-AXS APEX2 diffractometer with a CCD area detector (Mo K$\alpha$; $\lambda = 0.71073$ Å, graphite monochromator): frames were collected at $T = 93$ K or 103 K with $\omega$ and $\phi$ rotation at 5 or 10 s per frame. The measured intensities were reduced to $F^2$ and corrected for absorption with SADABS (SAINT-NT [33]). Structure solution, refinement and data output were carried out with the SHELXTL program package [34]. All non-hydrogen atoms were refined anisotropically. With the exception of the amino hydrogens in the structures **3a**, **2** and **3** all other hydrogens were included in the models in calculated positions and were refined as constrained to bonding atoms. The X-ray diffraction data collection of **1a** were collected on a CAD4 diffractometer in the $\omega$–$2\theta$ scan mode (Cu K$\alpha$; $\lambda = 1.5418$ Å, graphite monochromator). The SHELXS-97 program was applied for structure solution, while the SHELXL-97 was used for structure refinement [35]. All data were corrected for Lorentz and polarization effects.

## 3. Results and discussion

### 3.1. Synthesis

The macrocyclic **1** (Scheme 1) was synthesized via the cyclocondensation route [36] starting form 2-methoxybenzylideneacetone and ethylenediamine [32]. Subjection of **1** to a sodium borohydride reduction yielding the substituted cyclam **2** [32]. Reaction of **2** with picolyl chloride hydrochloride and sodium hydroxide gave the cyclam derivative **3**. The complexes **1a**, **2a** and **3a** were prepared from the respective macrocycles (**1**–**3**) with $Cu(ClO_4)_2 \cdot 6H_2O$ in methanolic solution.

### 3.2. X-ray structural study

In order to investigate, how complex formation mutually affects molecular conformations, we performed both crystal structure determination of the free macrocyclic ligands and their complexes with Cu(II) perchlorate.

Crystal data and selected experimental details are summarized in Table 1. Perspective views of the structures including the numbering schemes of relevant atoms are shown in Figs. 1, 3, 5, 7, 9 and 11. Packing illustrations are presented in Figs. 2, 4, 6, 8, 10 and 12. Geometric parameters of the co-ordinative interactions are given in Table 2.

#### 3.2.1. Crystal structure of *1* and *1a* [*1* $\cdot$ *Cu(ClO$_4$)$_2$*]

The X-ray crystallographic analysis of the macrocyclic diimine **1** yields the orthorhombic space group $P2_12_12_1$. Obviously, under the chosen conditions of crystal growing spontaneous optical resolution occurs, so that a given crystal consists of molecules of the same absolute configuration, which is *R*,*R* or *S*,*S* at the chiral centers C(1) and C(6) (Fig. 1a). The mean planes of the two C-N=C–C ring fragments are oriented at an angle of nearly 50° to each other inducing a boat-like conformation which forces the two exocyclic methyl groups into a *syn*-diequatorial arrangement. The aromatic rings are inclined with an angle of 40.9° towards each other. Moreover, as illustrated by the space filling model (Fig. 1b), partial collapsing of the intramolecular cavity leaves only a small 'hole' of approximately $2.6 \times 2.8$ Å being defined by the four nitrogen atoms. The fact, that neither significant conventional hydrogen bonds [37] nor weak directional contacts like C–H$\cdots\pi$ [38,39] and $\pi\cdots\pi$ interactions [40,41] are found in the crystal structure suggests that the strongly bent and compact shape of the molecule follows close-packing requirements. Thus, the crystal packing of **1** (Fig. 2) is characterized by an intensive nesting of molecules with the methoxy substituents and the voids of adjacent molecules gearing together.

Crystallization of the complex **1a** from acetonitrile/$H_2O$ yields violet crystals of the non-centrosymmetric space group *Pn*. Due to the presence of a glide plane, the crystal

Table 1
Crystallographic and structure refinement data of the compounds studied

| Compound | **1** | **1a** | **2** | **2a** | **3** | **3a** |
|---|---|---|---|---|---|---|
| Empirical formula | $C_{26}H_{36}N_4O_2$ | $C_{26}H_{36}N_4O_{10}CuCl_2$ | $C_{26}H_{40}N_4O_2$ | $C_{26}H_{40}N_4O_{10}CuCl_2$ | $C_{26}H_{36}N_4O_2 \cdot 2CHCl_3$ | $C_{38}H_{50}N_6O_{10}CuCl_2$ |
| Formula weight | 436.60 | 699.04 | 440.62 | 703.06 | 861.58 | 885.28 |
| Crystal system | orthorhombic | monoclinic | monoclinic | monoclinic | triclinic | monoclinic |
| Space group | $P2_12_12_1$ | $Pn$ | $P2_1/n$ | $P2_1/n$ | $P\bar{1}$ | $P2_1/n$ |
| $a$ (Å) | 8.0569(3) | 9.455(2) | 7.5373(2) | 17.8549(6) | 8.6908(2) | 8.9596(2) |
| $b$ (Å) | 13.2765(7) | 13.833(2) | 14.8712(5) | 9.1070(3) | 9.1665(3) | 12.8072(2) |
| $c$ (Å) | 22.5701(8) | 11.765(2) | 11.1425(4) | 19.5525(8) | 13.6417(4) | 16.7692(2) |
| $\alpha$ (°) | 90.0 | 90.0 | 90.0 | 90.0 | 89.295(2) | 90.0 |
| $\beta$ (°) | 90.0 | 93.18(3) | 99.931(2) | 107.507(1) | 75.642(1) | 95.322(1) |
| $\gamma$ (°) | 90.0 | 90.0 | 90.0 | 90.0 | 87.870(1) | 90.0 |
| $V$ (Å$^3$) | 2414.27(18) | 1536.4(5) | 1230.23(7) | 3032.06(19) | 1052.08(5) | 1915.93(8) |
| $Z$ | 4 | 2 | 2 | 4 | 1 | 2 |
| $F$(000) | 952 | 726 | 480 | 1468 | 452 | 926 |
| $D_c$ (Mg m$^{-3}$) | 1.201 | 1.511 | 1.189 | 1.540 | 1.360 | 1.535 |
| $\mu$ (mm$^{-1}$) | 0.077 | 0.945 | 0.076 | 0.958 | 0.451 | 0.777 |
| Data collection | | | | | | |
| Temperature (K) | 93(2) | 298(2) | 103(2) | 103(29) | 93(2) | 93(2) |
| Number of collected reflections | 18134 | 3539 | 14433 | 36331 | 61353 | 40344 |
| Within the $\theta$-limit (°) | 2.4–29.8 | 2.3–27.0 | 2.7–28.5 | 1.4–29.5 | 2.2–40.5 | 2.4–31.9 |
| Index ranges $\pm h$, $\pm k$, $\pm l$ | −11/9, −16/17, −31/31 | 0/12, 0/17, −15/14 | −5/10, −19/19, −14/13 | −24/13, −11/12, −25/27 | −15/15, −16/16, −24/24 | −13/13, −19/18, −23/24 |
| Number of unique reflections | 6480 | 3539 | 3076 | 8367 | 13414 | 6544 |
| $R_{int}$ | 0.0738 | 0.0000 | 0.0439 | 0.0450 | 0.0263 | 0.0342 |
| Refinement calculations | full-matrix least-squares on $F^2$ values | full-matrix least-squares on $F^2$ values | full-matrix least-squares on $F^2$ values | full-matrix least-squares on $F^2$ values | full-matrix least-squares on $F^2$ values | full-matrix least-squares on $F^2$ values |
| Weighting expression $w$[a] | $[\sigma^2(F_o^2) + (0.0490P)^2 + (0.0000P)^{-1}]$ | $[\sigma^2(F_o^2) + (0.0967P)^2 + (0.0000P)^{-1}]$ | $[\sigma^2(F_o^2) + (0.1000P)^2 + (0.0000P)^{-1}]$ | $[\sigma^2(F_o^2) + (0.1131P)^2 + (12.8379P)^{-1}]$ | $[\sigma^2(F_o^2) + (0.0524P)^2 + (0.3052P)^{-1}]$ | $[\sigma^2(F_o^2) + (0.0000P)^2 + (0.0000P)^{-1}]$ |
| Number of refined parameters | 293 | 401 | 163 | 443 | 252 | 265 |
| Number of $F$ values used [$I > 2\sigma(I)$] | 4016 | 2003 | 2022 | 5302 | 10123 | 5529 |
| Final $R$-indices | | | | | | |
| $R(=\sum\|\Delta F\|/\sum\|F_o\|)$ | 0.0598 | 0.0617 | 0.0530 | 0.0785 | 0.0408 | 0.0419 |
| $wR$ on $F^2$ | 0.1308 | 0.1708 | 0.1676 | 0.2299 | 0.1128 | 0.0739 |
| $S$(=Goodness of fit on $F^2$) | 1.014 | 0.984 | 1.031 | 0.992 | 0.984 | 0.956 |
| Final $\Delta\rho_{max}/\Delta\rho_{min}$ (e Å$^{-3}$) | 0.23/−0.46 | 0.84/−0.53 | 0.45/−0.21 | 0.87/−0.96 | 1.282/−0.986 | 1.09/−0.94 |

[a] $P = (F_o^2 + 2F_c^2)/3$.

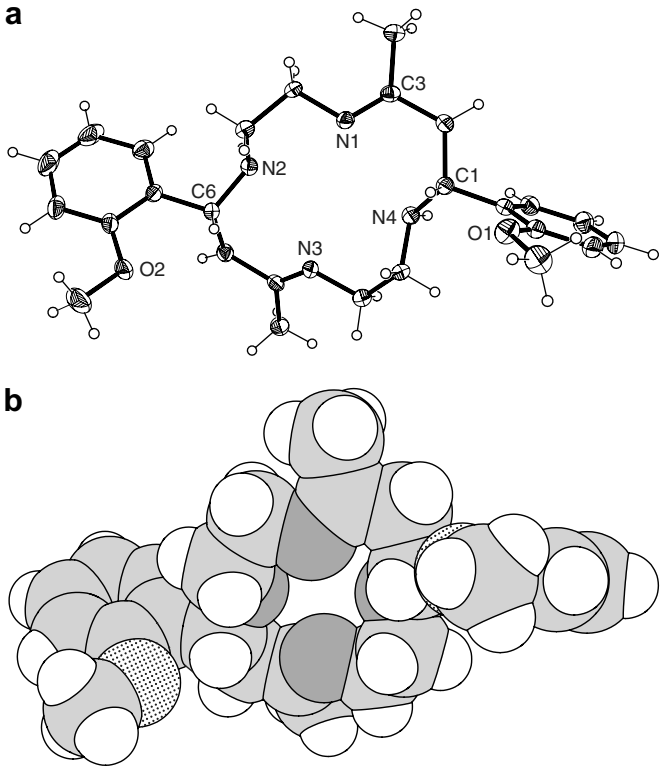


Fig. 1. (a) Molecular structure with atom labelling of relevant atoms and displacement ellipsoids at the 40% probability level and (b) space filling model of **1**.

Table 2
Structural parameters (distances/Å, angles/°) involving co-ordinative interactions of complexes **1a**, **2a** and **3a**

| Atoms involved | **1a** | **2a** | **3a** |
|---|---|---|---|
| Cu(1)–N(1) | 1.966(12) | 2.015(4) | 2.036(1) |
| Cu(1)–N(2) | 1.975(11) | 2.038(3) | 2.106(1) |
| Cu(1)–N(3) | 2.032(10) | | 2.517(1) |
| Cu(1)–N(4) | 1.979(11) | | |
| Cu(1)–O(1) | 2.574(10) | 2.562(3) | |
| Cu(1)–O(5) | 2.976(11) | | |
| Cu(2)–N(1A) | | 2.022(3) | |
| Cu(2)–N(2A) | | 2.029(3) | |
| Cu(2)–O(1A) | | 2.363(4) | |
| N(1)–Cu(1)–N(2) | 94.7(5) | 93.2(1) | 86.5(1) |
| N(1)–Cu(1)–N(3) | 175.8(6) | | 91.3(1) |
| N(2)–Cu(1)–N(4) | 177.7(5) | | |
| N(1)–Cu(1)–N(4) | 85.7(4) | | |
| N(2)–Cu(1)–N(3) | 87.8(5) | | 78.5(1) |
| N(3)–Cu(1)–N(4) | 91.7(4) | | |
| O(1)–Cu(1)–O(5) | 163.6(5) | | |
| O(1)–Cu(1)–N(1) | 88.2(5) | | |
| O(1)–Cu(1)–N(2) | 90.4(5) | | |
| O(1)–Cu(1)–N(3) | 95.2(4) | | |
| O(1)–Cu(1)–N(4) | 91.8(5) | | |
| O(5)–Cu(1)–N(1) | 71.5(5) | | |
| O(5)–Cu(1)–N(2) | 91.0(6) | | |
| O(5)–Cu(1)–N(3) | 105.1(4) | | |
| O(5)–Cu(1)–N(4) | 86.9(5) | | |
| N(1A)–Cu(2)–N(2A) | | 88.5(1) | |
| O(1A)–Cu(2)–N(1A) | | 101.9(1) | |
| O(1A)–Cu(2)–N(2A) | | 89.8(1) | |

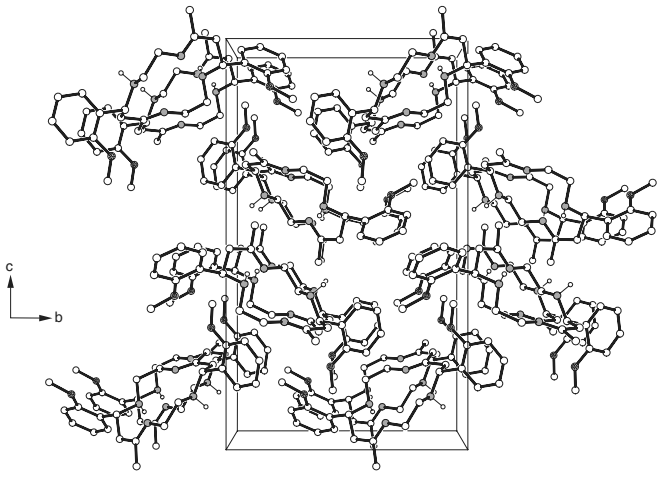


Fig. 2. Packing structure of **1** with carbon-bonded hydrogen atoms omitted.

consists of a racemic mixture of stereoisomers of the configuration *R*,*R* and *S*,*S* while the meso *R*,*S*-stereoisomer has not been found in the crystalline form. The amino hydrogens H(1′) and H(3′) of **1a** are located on one side of the macrocycle. Since they contact to the ether oxygens of the anisyl residues, their methoxy groups exhibit a *syn*-arrangement (Fig. 3). Another interesting structural feature of **1a** can be seen in the highly distorted coordination sphere of the copper ion, which is reflected by unequal Cu–O bond lengths and the O–Cu–O angle that deviates significantly from linearity (163.6°). The Cu–O distances of 2.574(10) and 2.976(11) Å also indicate rather weak coordination of the anions to the copper center. The Cu–N($sp^2$) distances [1.975(11), 1.979(11) Å] and the Cu–N($sp^3$) bond lengths [1.966(12), 2.032(10) Å] are in the same order of magnitude. The high degree of conformational distortion can be attributed to the different binding behavior of the two perchlorate anions. One of them is

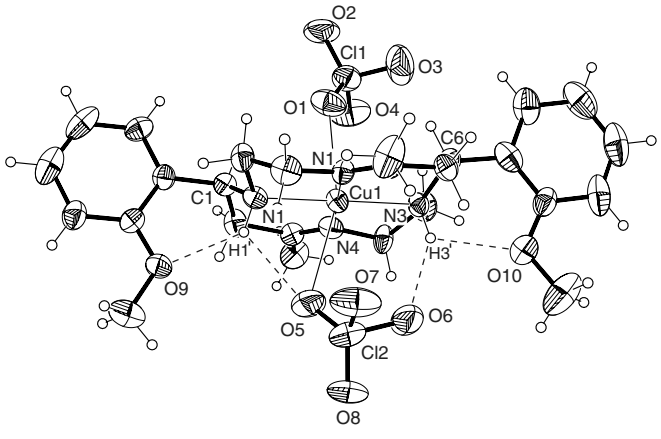


Fig. 3. Molecular structure of **1** · $Cu(ClO_4)_2$ with atom labelling of relevant atoms and displacement ellipsoids at the 40% probability level. Only one site of the disordered perchlorate ions is displayed. Broken lines represent hydrogen bond type contacts.

primarily associated to the ligand via intramolecular N–H···O contacts (O···H 2.243, 2.302 Å), while the other one is involved in intermolecular C–H···O hydrogen bonding (O···H 2.495, 2.664 Å) [42,43]. The crystal packing of **1a** is composed of molecular layers running parallel to the crystallographic B-plane (Fig. 4). They are held together by weak C–H···O hydrogen bond type contacts (O···H 2.49 Å) and π···π stacking interactions between the aromatic groups. The interlayer association is accomplished by the perchlorate ions that form weak interactions to arene and methylene hydrogens.

Previous papers have been published on metal complexes formed by the unsubstituted diphenyl analogue of **1** [21,29]. The crystal structure of the $Ni(ClO_4)_2$ complex [29], in which the diimine ligand has the same chirality as in **1a**, shows that the absence of the methoxy groups does not much effect the molecular conformation. On the other hand, the Ni(II) cation induces significant changes in coordination behavior compared to the Cu(II) in **1a**. Only one of the perchlorate ions occupies an axial position with both N–H groups oriented towards the opposite side of the $NiN_4$ plane, forming N–H···O hydrogen bonds to oxygen atoms of different perchlorate ions. Thus, a totally different molecular assembly within the crystal results.

### 3.2.2. Crystal structure of **2** and **2a** [**2** · $Cu(ClO_4)_2$]

The macrocyclic tetraamine **2** yields colorless crystals of the monoclinic space group $P2_1/n$ with two molecules within the unit cell. The torsion angles along the macroring are all ±*gauche* and *anti*. Although not all of them adopt idealized values (−66.0°, 175.4°, −175.2°, 69.6°, 168.3°, −168.8°, 72.8°), the macrocycle shows a regular, less strained conformation (Fig. 5). With the exception of the axial amino hydrogens H(2′), which for sterical reasons are not associated, all other strong donors and acceptors are involved in intramolecular hydrogen bonding. Two of the N–H bonds are directed towards the ring center, which opens the possibility of forming asymmetrical bifurcated hydrogen bonds [37] of the N–H···N type [N(1)–H(1′)···N(2) 2.32 Å, 135.0°; N(1)–H(1′)···N(2A) 2.57 Å, 110.7°], thus giving a cyclic four-membered hydrogen bond motif inside the macroring. As a consequence, van der Waals type interactions primarily contribute to the stabilization of the columnar packing mode of compound **2** (Fig. 6). Former investigations have shown that reduction of the unsubstituted diphenyl analogue of the diimine **1** yields the three possible stereo isomeric tetraazacyclotetradecanes in ca. 85:15:1 ratio [44,45]. The major product,

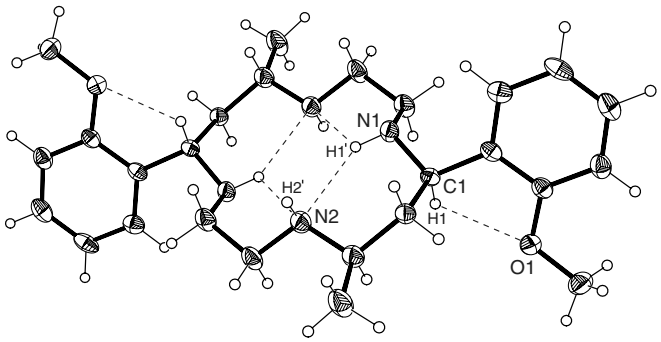


Fig. 5. Perspective view of **2** with numbering of relevant atoms and displacement ellipsoids at the 40% probability level. Broken lines represent hydrogen bond type contacts.

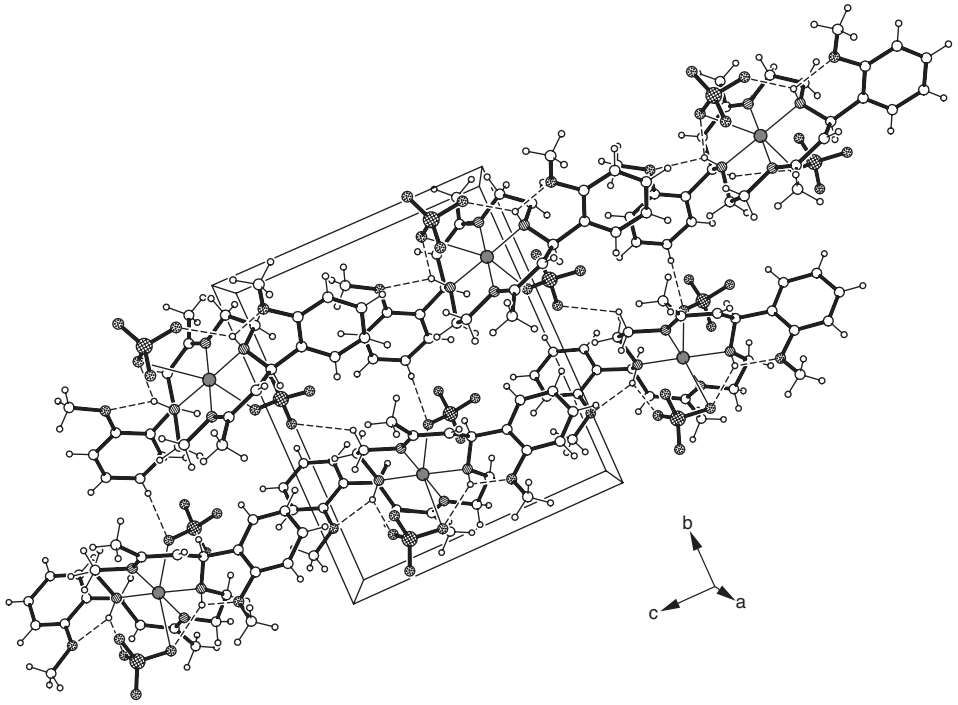


Fig. 4. Packing illustration of **1** · $Cu(ClO_4)_2$. Non-relevant hydrogen atoms are omitted for clarity.

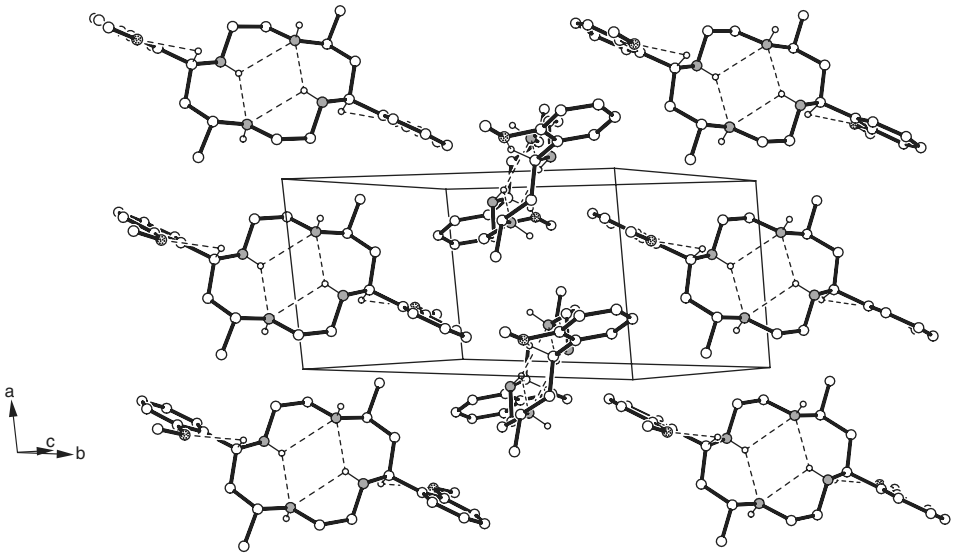


Fig. 6. Packing structure of **2**. Non-relevant hydrogen atoms are omitted for clarity.

which has been characterized by X-ray analysis [46] agrees with the configuration found for **2**.

Crystallization of complex **2a** from acetonitrile/$H_2O$ yields crystals of the monoclinic space group $P2_1/c$ with two crystallographically independent halves of molecules in the asymmetric unit of the cell (Fig. 7), i.e. the copper atoms are located on crystallographic inversion centers (1/2, 1/2, 0 and 1, 0, 0). In both molecules, the anions are disordered over two sites. The Cu(II) exhibits an elongated octahedral coordination environment with the axial positions being occupied by one oxygen atom of each perchlorate ion. In one of the complexes, the Cu–O distance is rather long [2.562(3) Å] indicating only a weak binding, while in the second complex the respective bond is 2.363(4) Å. The Cu–N bond lengths [2.015(4)–2.038(3) Å] are within the expected range [7]. The six-membered chelate rings of the complex molecules adopt a distorted chair-like conformation with the anisyl and methyl substituents in equatorial positions, whereas the five-membered chelate rings are twisted. The aromatic units are arranged nearly perpendicular (88.4°, 86.7°) with respect to the $CuN_4$-plane. Although the independent molecules have similar conformations, they deviate in their mode of interactions. In molecule 1, the atom H(1′) forms an intramolecular bifurcated hydrogen bond [37] to the oxygens O(2) (2.245 Å) of the perchlorate anion and O(5) (2.225 Å) of

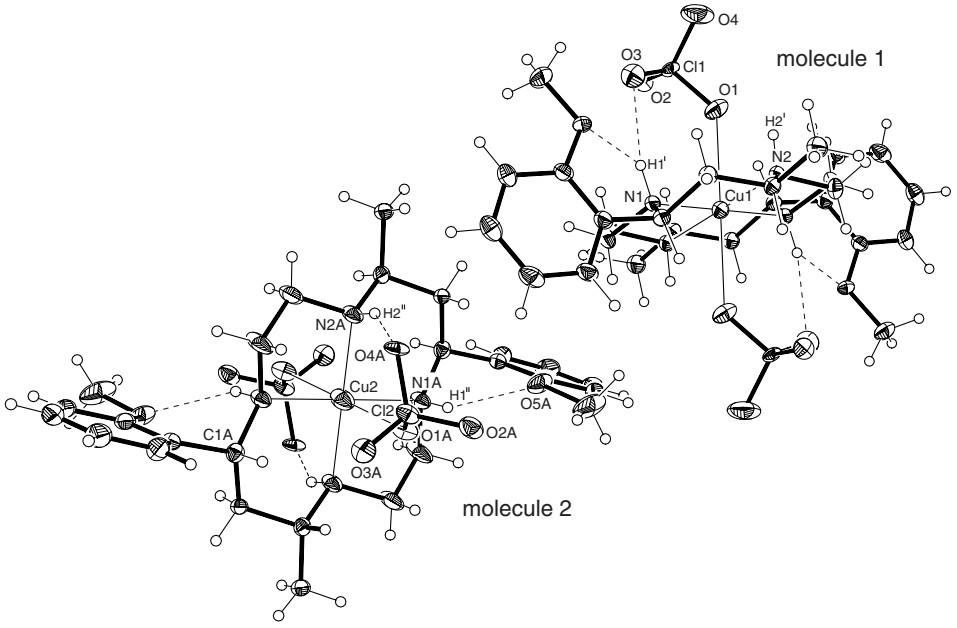


Fig. 7. Molecular structure of **2** · $Cu(ClO_4)_2$ with numbering of relevant atoms and displacement ellipsoids at the 40% probability level. Only one site of the disordered perchlorate ions is displayed. Broken lines represent hydrogen bond type contacts.

the anisyl group, while H(2′) remains free. In molecule 2, all amino hydrogens participate in intramolecular hydrogen bonding [H(1″)···O(1A) 2.284 Å, H(2″)···O(4A) 2.196 Å]. The packing of the crystals consists of infinite molecular chains extending in direction of the crystallographic *c*-axis (Fig. 8). Within these chains, the basal planes of consecutive molecules are titled to each other with an angle of 52.5° thus allowing formation of intermolecular C–H···O hydrogen bonds (O···H 2.200, 2.562 Å) between the anions and methyl groups of the ligands.

### 3.2.3. Crystal structure of $\mathbf{3}\cdot 2CHCl_3$ and **3a** [$\mathbf{3}\cdot Cu(ClO_4)_2$]

Crystals of compound **3**, suitable for diffraction experiments, could only be obtained as 1:2 (host:guest) solvent complex with chloroform (space group $P\bar{1}$). The unit cell of the crystal contains one complex entity (Fig. 9) with the solvent molecules associated via C–H···N hydrogen bond type interactions [42,43] with the pyridyl nitrogen [N(3)···H(1G) 2.37 Å]. Also in the present case, intramolecular contacts contribute to the molecular conformation. The hydrogen atom attached to N(2), the position of which could be gained from the difference electron density map, is directed towards the interior of the ring, and its well-defined N–H···N geometry suggests the existence of a weak hydrogen bridge to N(1) [N(2)–H(2′)···N(1) 2.25 Å, 137.7°]. The packing structure of the solvent complex of

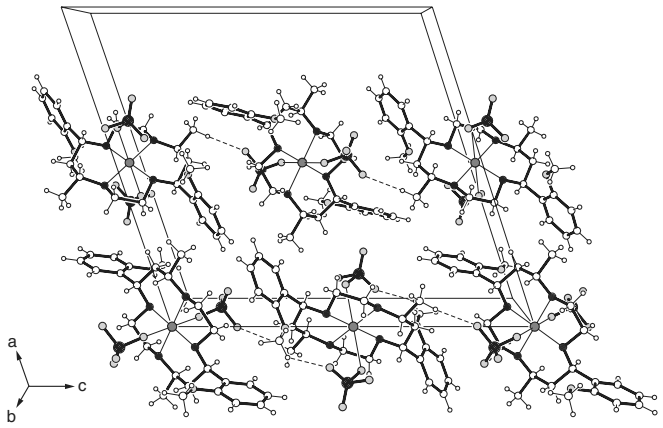


Fig. 8. Packing illustration of $\mathbf{2}\cdot(ClO_4)_2$.

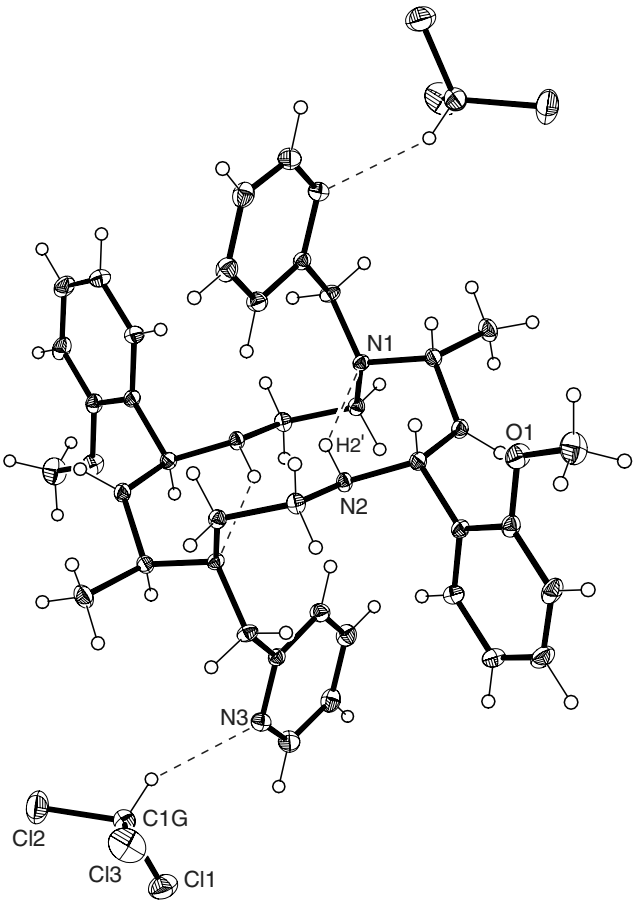


Fig. 9. Perspective view of the host–guest unit $\mathbf{3}\cdot CHCl_3$ (1:2) with numbering of relevant atoms and displacement ellipsoids at the 40% probability level. Hydrogen bond type contacts are displayed as broken lines.

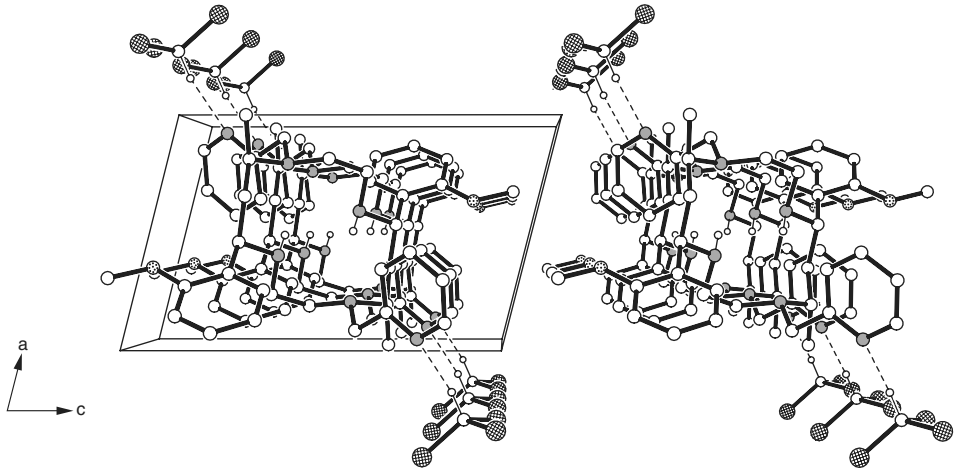


Fig. 10. Packing diagram of $\mathbf{3}\cdot CHCl_3$ (1:2). Non-relevant hydrogen atoms are omitted for clarity.

**3** is composed of discrete **3** · $CHCl_3$ 1:2 aggregates stacked in a columnar array along the crystallographic *b*-axis (Fig. 10). Within the stacks, the host molecules are associated by aromatic edge-to-face (C–H···π) contacts [38,39] with the electron deficient pyridyl residues acting as donors and the electron-rich anisyl groups as hydrogen bond acceptors. The distance between the *para* C–H hydrogen of the pyridine and the ring centroid of the anisyl is 2.53 Å, while the C–H···centroid angle is 152.2°.

The Cu(II) complex **3a** yields blue crystals of the monoclinic space group $P2_1/n$ when crystallized from methanol. The asymmetric unit of the cell contains one half of the molecule with the copper atom located on the symmetry center 1/2, 1, 0. Different from structures **1a** and **2a**, the perchlorate ions of **3a** are not involved in complexation (Fig. 11). Instead, the nitrogen atoms of the two pyridylmethyl substituents occupy the apical sites of the octahedral coordination polyhedron. The axial Cu–N distances are 2.517(1) Å, whereas the equatorial Cu–N bonds are 2.036(1) and 2.106(1) Å. For steric reasons, the planes of the pyridyl residues are inclined at an angle of 54.3° with respect to the $CuN_4$ basal plane. Although rich in strong hydrogen bond acceptors, the anions show only poor association. Obviously, shielding of the amino hydrogens by the 2-picolyl units prevents effective hydrogen bonding to the counter ions. The same co-ordination behavior is also found in reported structures of copper(II) complexes having a similar pyridyl-substituted cyclam framework but differ in the mode of substitution [25–28]. It is also interesting to compare the structure of **3a** with the crystal structure of the copper(II) complex of the *N*-acetyl diphenyl substituted cyclam derivative reported previously [24]. In this structure, the charged carboxylate oxygens act as apical coordination sites of the *trans*-octahedral coordination environment of Cu(II). In addition, two ethanol molecules are hydrogen bonded to the two coordinated carboxyl oxygens thus preventing further intermolecular contacts.

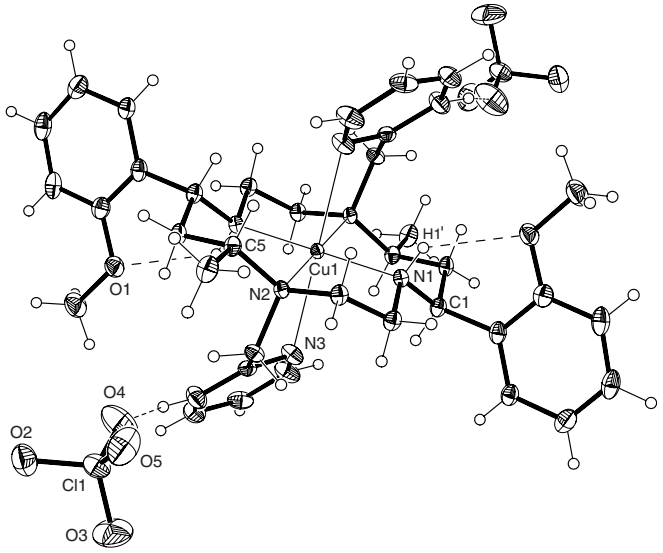


Fig. 11. Molecular structure of **3** · $Cu(ClO_4)_2$ with numbering of relevant atoms and displacement ellipsoids at the 40% probability level. Broken lines represent hydrogen bond type interactions.

The packing structure of **3a** is characterized by two-dimensional layers of complex cations which are stacked along the crystallographic *c*-axis (Fig. 12). The arrangement is stabilized by perchlorate ions, which fill the interstitial spaces between the layers and bridge the cations by weak C–H···O contacts (O···H 2.34–2.58 Å) [42,43]. Aromatic π···π interactions [40,41] are formed within the layers. The interacting aryl groups are displaced relative to each other, showing centroid–centroid distances of 4.50 Å for the phenyl rings and 4.30 Å for coordinated pyridyl

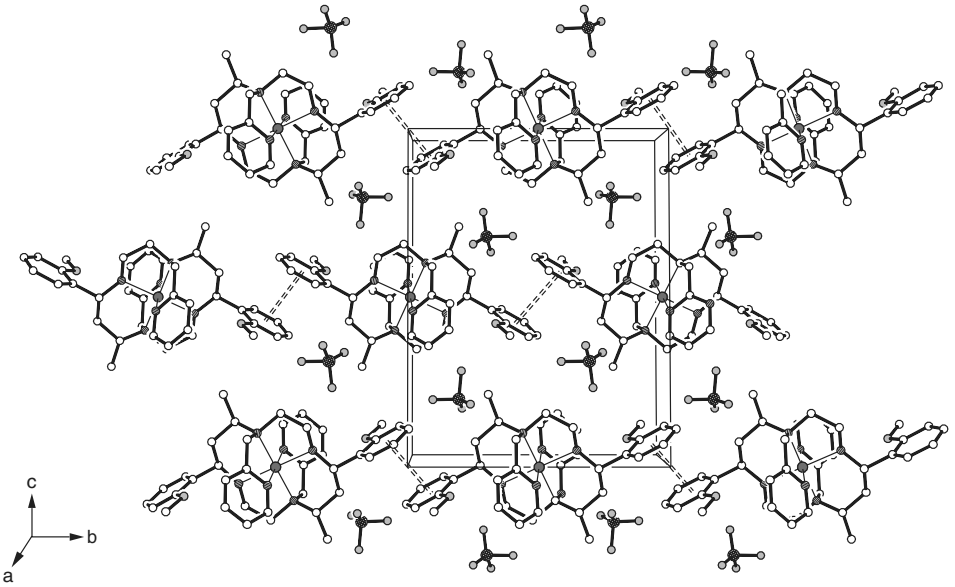


Fig. 12. Packing illustration of **3** · $Cu(ClO_4)_2$ with aromatic π–π interactions depicted as broken double lines. All hydrogen atoms are omitted for clarity.

fragments. Other types of non-covalent cation–cation interactions are not observed in the crystal.

## 4. Conclusion

A comparative structural study involving a designed series of cyclam type derivatives **1**–**3** that feature a different degree of saturation, and thus flexibility of the macroring, different number of functional appendages, and thus power of coordination, including their respective complexes with Cu(II) perchlorate has been reported.

X-ray crystal structures of the uncomplexed macrocycles **1**–**3** reveal that steric shielding caused by the ring substituents prevents the amino hydrogens from forming effective non-covalent bonding between molecules. Instead, these donors are either free or are used for intramolecular hydrogen bonding. The unsaturated diimine macrocycle **1** crystallizes in a non-centrosymmetric crystal structure. According to the given space group, a selected crystal contains molecules of the same absolute configuration and therefore is optically active. The strongly distorted geometry with a nearly complete collapsing of the macrocyclic cavity means that no intramolecular hydrogen bonds are present. In the case of **2**, two of the amino hydrogens are directed to the interior of the macrocycle giving a four-membered system of bifurcated hydrogen bonds, which is also found in crystal structures of related cyclam derivatives [22,23]. Intramolecular hydrogen bonding of the *N*-substituted macrocyclic ring is also found in the 1:2 inclusion compound of **3** with chloroform. However, only two bent N–H···N hydrogen bonds are present giving the molecule a pseudo-tricyclic structure.

In the complexes **1a**–**3a**, the metal center exhibits a more or less distorted octahedral coordination environment in which the four macroring nitrogens define the equatorial coordination sites of the polyhedron. Nevertheless, the ligand molecules show marked differences in their complexing behavior. The cyclam-based copper(II) complexes **2a** and **3a** show centrosymmetric molecular structures in the solid state. As expected, the apical coordination sites in **2a** are occupied by the oxygen atoms of two perchlorate anions [47]. A second oxygen of each anion forms an intramolecular N–H···O hydrogen bond to the complexed macroring. The presence of two *N*-substituted chelating pyridine containing pendants in the macrocycle **3** affects a different mode of coordination of the complex **3a** which is now of the $CuN_6$ type. As a result, its crystal structure consists of discrete complex cations and perchlorate anions which are cross-linked by weak C–H···O hydrogen bonds. The fact that the gross structure of **3a** corresponds to reported copper(II) complexes of related pyridyl-substituted cyclams [25–28] suggests rather robust conformational behavior of the macroring, including the pyridyl side arms, even in the presence of other potentially co-ordinating pendants such as the anisyl residues in **3a**, indicating particular co-ordinative interaction of this system. Similar to the uncomplexed diimine macroring **1**, the crystal structure of the respective complex **1a** has also an enantiomorphous configuration attributed to the *R*,*R* or *S*,*S* configuration at the chiral C atoms. Obviously, the reduced number of strong hydrogen bond donors, which is only half of those found in the complexes **2a** and **3a** and which determine the degree of cation–anion interactions, results in a less symmetric boat-like geometry of the complexed macrocycle.

Thus, only the pyridine containing pendants in **3a** proved effective in coordination of the metal ion while the uncomplexed macrocycle **3** yielded an inclusion compound with chloroform, also indicating a special ability relating to this series of compounds.

## 5. Supplementary data

Full details of the crystal structure analyses of **1**, **2**, **3**, **1a, 2a** and **3a** have been deposited with the Cambridge Crystallographic Data Centre (CCDC Nos. 288907–288909 and 288904–288906, respectively). Copies may be obtained free of charge on application to the Director, CCDC, 12 Union Road, Cambridge CB2 1EZ, UK [fax (int. code): +44 1223 336 033, e-mail: deposit@ccdc.cam.ac.uk].

## Acknowledgements

We gratefully acknowledge financial support by the firms of Hoechst and Clariant, as well as the Fonds der Chemischen Industrie.

## References

[1] J.L. Atwood, J.E.D. Davies, D.D. MacNicol, F. Vögtle (Eds.), Comprehensive Supramolecular Chemistry, vol. 1, Elsevier, Oxford, 1996.
[2] L.F. Lindoy, The Chemistry of Macrocyclic Ligand Complexes, Cambridge University Press, Cambridge, 1989.
[3] P.G. Potvin, J.M. Lehn, in: R.M. Izatt, J.J. Christensen (Eds.), Synthesis of Macrocycles – The Design of Selective Complexing Agents, Progress in Macrocyclic Chemistry, vol. 3, Wiley, New York, 1987, p. 167.
[4] A. Bianchi, K. Bowman-James, E. Garcia-Espana (Eds.), Supramolecular Chemistry of Anions, Wiley–VCH, Weinheim, 1997.
[5] K. Gloe (Ed.), Macrocyclic Chemistry, Springer, Dordrecht, 2005.
[6] W. Niu, E.H. Wong, G.R. Weisman, Y. Peng, C.J. Anderson, L.N. Zakharov, J.A. Golen, A.I. Rheingold, Eur. J. Inorg. Chem. (2004) 3310.
[7] T. Schönherr, E. Weber, W. Seichter, Z. Anorg. Allg. Chem. 627 (2001) 2420.
[8] R.I. Haines, Rev. Inorg. Chem. 21 (2002) 165.
[9] K.P. Wainwright, Coord. Chem. Rev. 166 (1997) 35.
[10] J. Costamagna, G. Ferraudi, B. Matsuhiro, M. Campos-Vallette, J. Canals, M. Villagráu, J. Vargas, M.J. Aguirre, Coord. Chem. Rev. 196 (2000) 125.
[11] B. Korybut-Daszkiewicz, J. Taraszewska, K. Zieba, A. Makal, K. Wozniak, Eur. J. Inorg. Chem. (2004) 3335.
[12] K.S. Miu, M.P. Suh, Chem. Eur. J. 7 (2001) 303.
[13] T. Schönherr, E. Weber, W. Seichter, J. Incl. Phenom. 50 (2004) 187.
[14] J.S. Bradshaw, K.E. Krakowiak, R.M. Izatt, Aza-Crown Macrocycles, Wiley, New York, 1993.
[15] E. Weber, in: J.L. Atwood, J.W. Steed (Eds.), Encyclopedia of Supramolecular Chemistry, Marcel Dekker, New York, 2004, p. 261.

[16] J.W. Steed, J.L. Atwood, Supramolecular Chemistry, Wiley, Chichester, 2000.
[17] E. Brucher, A.D. Sherry, in: A.E. Merbach, E. Toth (Eds.), The Chemistry of Contrast Agents in Medical Magnetic Resonance Imaging, Wiley, New York, 2001 (Chapter 6).
[18] J.W. Siebert, A.H. Cory, J.G. Cory, Chem. Commun. (2002) 154.
[19] X. Liang, J.A. Parkinson, M. Weishäupl, R.O. Gould, S.J. Paisey, H.-S. Park, T.M. Hunter, C.A. Blindauer, S. Parsons, P.J. Sadler, J. Am. Chem. Soc. 124 (2002) 9105.
[20] C. Saudan, V. Balzani, M. Gorka, S.-K. Lee, J. van Heyst, M. Maestri, P. Ceroni, V. Vicinelli, F. Vögtle, Chem. Eur. J. 10 (2004) 899.
[21] D.F. Cook, N.F. Curtis, R.W. Hay, J. Chem. Soc., Dalton Trans. (1973) 1160.
[22] P.W.R. Caulkett, D. Greatbanks, R.W. Turner, Heterocycles 9 (1978) 1003.
[23] Z. Urbanczyk-Lipkowska, J.W. Krajewski, P. Gluzinski, G.D. Andretti, G. Bocelli, Acta Crystallogr., Sect. B 37 (1981) 470.
[24] L. Chen, L.K. Thompson, J.N. Bridson, J. Xu, S. Ni, R. Guo, Can. J. Chem. 71 (1993) 1805.
[25] S.-G. Kang, S.-J. Kim, J.H. Jeong, Polyhedron 17 (1998) 3227.
[26] K.-Y. Choi, K.-M. Chun, I.-H. Suh, Polyhedron 18 (1999) 2811.
[27] K.-Y. Choi, H.-O. Lee, Y.-S. Kim, K.-M. Chun, K.-C. Lee, S.-N. Choi, C.-P. Hong, Y.-Y. Kim, Inorg. Chem. Commun. 5 (2000) 496.
[28] A.E. Goeta, J.A.K. Howard, D. Maffeo, H. Puschmann, J.A.G. Williams, D.S. Yufit, J. Chem. Soc., Dalton Trans. (2000) 1873.
[29] N.F. Curtis, D.C. Weatherburn, Acta Crystallogr., Sect. E 58 (2002) m423.
[30] J. Leonard, B. Lygo, G. Procter, Praxis der Organischen Chemie, Wiley–VCH, New York, 1996.
[31] I.M. Heilbron, J.S. Buck, J. Chem. Soc. (1921) 1509.
[32] K. Hideg, D. Lloydt, J. Chem. Soc., Sect. C (1971) 3441.
[33] Bruker Analytical X-ray Systems, SAINT-NT Version 6.0, 2003.
[34] Bruker Analytical X-ray Systems, SHELXTL-NT Version 6.10, 2000.
[35] G.M. Sheldrick, SHELX-97: Program for Crystal Structure Solution and Refinement, University of Göttingen, Göttingen, Germany, 1997.
[36] N.F. Curtis, Coord. Chem. Rev. 3 (1968) 3.
[37] G.A. Jeffrey, An Introduction to Hydrogen Bonding, Oxford University Press, Oxford, 1997.
[38] M. Nishio, M. Hirota, Y. Umezawa, The CH/π Interaction, Evidence, Nature, and Consequences, Wiley–VCH, New York, 1998.
[39] M. Nishio, CrystEngComm 6 (2004) 130.
[40] E.A. Meyer, R.K. Castellano, F. Diederich, Angew. Chem. 115 (2003) 1244.
[41] E.A. Meyer, R.K. Castellano, F. Diederich, Angew. Chem., Int. Ed. 42 (2001) 1210.
[42] G.R. Desiraju, T. Steiner, The Weak Hydrogen Bond, IUCr Monographs on Crystallography, vol. 9, Oxford University Press, Oxford, 1999.
[43] M. Nishio, in: J.L. Atwood, J.W. Steed (Eds.), Encyclopedia of Supramolecular Chemistry, Marcel Dekker, New York, 2004, p. 1576.
[44] D.F. Cook, Ph.D. Thesis, Victoria University of Wellington, Wellington, New Zealand, 1972.
[45] G. Ferguson, P. Roberts, D. Lloyd, K. Hideg, J. Chem. Soc., Chem. Commun. (1977) 149.
[46] G. Ferguson, P.J. Roberts, R.W. Hay, D.P. Liplani, J. Chem. Res. 314 (1978) 3734.
[47] M. Melnik, M. Kabesova, L. Macaskova, C.E. Holloway, J. Coord. Chem. 45 (1998) 31.